


Hybrid van der Waals Epitaxy

Lin Hu^{1,2,3,*}, Danshuo Liu,⁴ Fawei Zheng,^{1,2} Xuelin Yang,^{4,†} Yugui Yao,^{1,2} Bo Shen,^{4,5} and Bing Huang^{3,6,‡}
¹Centre for Quantum Physics, Key Laboratory of Advanced Optoelectronic Quantum Architecture and Measurement (MOE),
 School of Physics, Beijing Institute of Technology, Beijing 100081, China
²Beijing Key Lab of Nanophotonics & Ultrafine Optoelectronic Systems, School of Physics,
 Beijing Institute of Technology, Beijing 100081, China
³Beijing Computational Science Research Center, Beijing 100193, China
⁴State Key Laboratory of Artificial Microstructure and Mesoscopic Physics,
 Nano-optoelectronics Frontier Center of Ministry of Education, School of Physics,
 Peking University, Beijing 100871, China
⁵Collaborative Innovation Center of Quantum Matter, Beijing 100871, China
⁶Department of Physics, Beijing Normal University, Beijing 100875, China

 (Received 1 January 2024; revised 13 May 2024; accepted 12 June 2024; published 24 July 2024)

The successful growth of non-van der Waals (vdW) group-III nitride epilayers on vdW substrates not only opens an unprecedented opportunity to obtain high-quality semiconductor thinfilm but also raises a strong debate for its growth mechanism. Here, combining multiscale computational approaches and experimental characterization, we propose that the growth of a nitride epilayer on a vdW substrate, e.g., AlN on graphene, may belong to a previously unknown model, named hybrid vdW epitaxy (HVE). Atomic-scale simulations demonstrate that a unique interfacial hybrid-vdW interaction can be created between AlN and graphene, and, consequently, a first-principles-based continuum growth model is developed to capture the unusual features of HVE. Surprisingly, it is revealed that the in-plane and out-of-plane growth are strongly correlated in HVE, which is absent in existing growth models. The concept of HVE is confirmed by our experimental measurements, presenting a new growth mechanism beyond the current category of material growth.

DOI: [10.1103/PhysRevLett.133.046102](https://doi.org/10.1103/PhysRevLett.133.046102)

Introduction—The ability to epitaxially grow large-scale crystalline thinfilm is not only critical to explore the intrinsic electronic and optoelectronic properties of materials, but also holds great promise for device manufacturing in the industry. In particular, tremendous efforts have been made to grow high-quality group-III nitride thinfilms [1–12], which are important candidates for developing advanced electronic and optoelectronic devices in the postsilicon age [13–18]. In parallel with the rapid experimental progress, significant interest has been made to understand the growth mechanism or optimize the growth model, to achieve epitaxial thinfilms with better quality and larger size [5–12].

The traditional models for thinfilm growth can be classified based on the principles of wetting or nonwetting [19,20], which are mainly determined by the binding energy (E_{binding}) between substrate and epilayer. For example, when the lattice mismatch between the epilayer and substrate is sufficiently small [Fig. 1(a)], the E_{binding} is negative and will increase (i.e., more negative) with the increased epilayer area size [Fig. 1(e)]. It means that the film first wets the substrate along the in-plane direction and

then grows in a layer-by-layer style [Fig. 1(a)], denoted as the Frank-van der Merwe (FV) model [20–22]. Oppositely, when the lattice mismatch between epilayer and substrate is sufficiently large [Fig. 1(b)], the film cannot wet the substrate and, consequently, the 3D islands instead of a continuous thinfilm will be formed. In this situation, the E_{binding} that is positive will increase (i.e., more positive) with the increased size [Fig. 1(e)], denoted as the Volmer-Weber (VW) model [19,20,23]. In reality, an intermediate case may exist between the FV and VW models, denoted as the Stranski-Krastanow (SK) model [Fig. 1(c)] [20,24], in which the trend of E_{binding} is similar to that of the FV one but with a smaller slope [Fig. 1(e)], indicating a lesser wetting effect. Consequently, the thinfilm will grow in the FV model at a smaller thickness but transfer to the VW model at a larger thickness [25,26]. Overall, as shown in Fig. 1(f), the existing models grow along either the in-plane or out-of-plane direction, i.e., the size (L) and the thickness (h) of the epilayer is always decoupled during growth.

Recently, intensive interest has arisen to develop a new type of growth mediated by the weak interfacial van der Waals (vdW) interaction, denoted as the vdW epitaxy (VE) [27–30], in which the requirement of a lattice match is lifted. Inspired by the VE model, the epitaxial growth of nitrides or halides on 2D substrates (e.g., graphene [4–12] or *h*-BN [2,12]) is proposed, opening a new door toward growing a

*Contact author: hulin@bit.edu.cn

†Contact author: xlyang@pku.edu.cn

‡Contact author: bing.huang@csrc.ac.cn

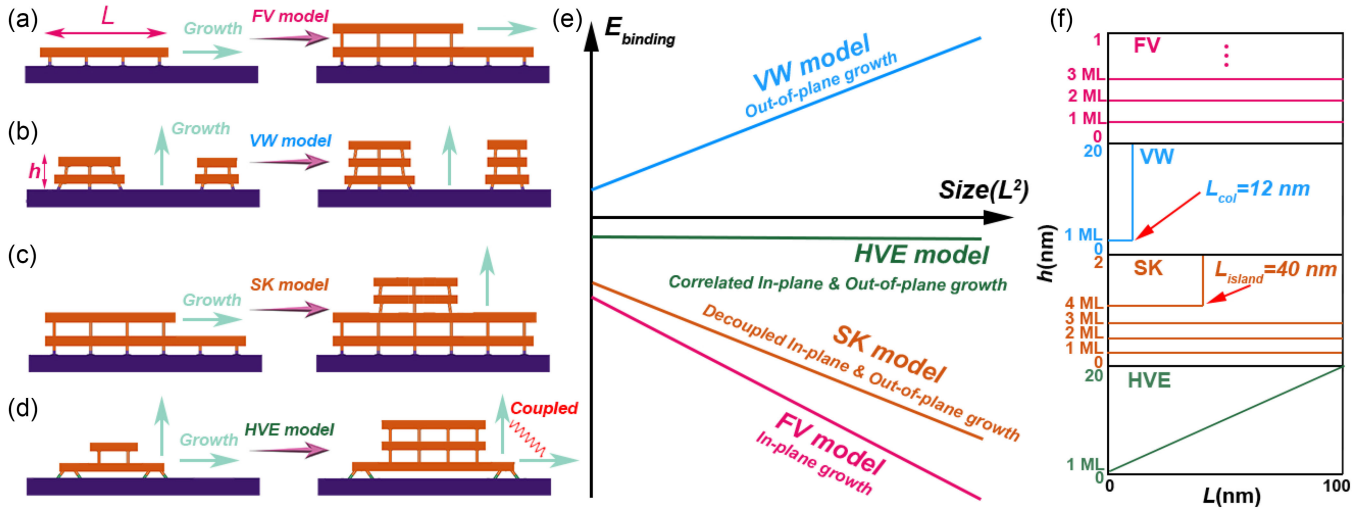


FIG. 1. Different growth models. (a) FV model. (b) VW model. (c) SK model. (d) HVE model. L and h indicate the edge length and thickness of growth islands, respectively. (e) Growth phase diagram as a function of E_{binding} (binding energy between substrate and epilayer) and L^2 (epilayer area size). FV, VW, SK, and HVE models are formed under different interfacial interactions. (f) Relationship between L and h for different growth models. In the FV model, the values of island size L and height h are adopted from CoO grown on MgO(100) at 673 K [21]. In the VW model, the values of columnar length L_{col} and height h are adopted from Ni grown on Si(100) at 300 K [23]. In the SK model, the values of island size L_{island} and height h are adopted from Ge grown on Si(100) at 600 K [24]. In the HVE model, the values of in-plane size L and height h are adopted from AlN grown on graphene. We note that it is more convenient for the VW model to be characterized by the formation of columnar structures. In the SK model, the increase of h may also affect the L of initial layers, as a result of the strain relaxation effect, which is not shown here.

high-quality non-vdW system on a vdW substrate. However, its growth mechanism raises great controversies: While some believe it belongs to the VE-like model with weak interfacial interaction [5–8], others believe it is an FV-like model with much stronger chemical bonding [10,11]. It is urgent to clarify the microscopic mechanism if people want to extend this new approach to grow many other thinfilms.

Here, combining multiscale simulations and experimental synthesis (see all the details in Method in the Supplemental Material [31]), surprisingly, we conclude that the growth of group-III nitride on a 2D substrate belongs to a previously unknown mode, denoted as hybrid vdW epitaxy (HVE). As shown in Fig. 1(d), due to the chemical inertness of 2D materials, the chemical bonds between the central area of nitride thinfilm and the 2D material will spontaneously break, leaving the bonds solely at the corners during growth. Consequently, an interfacial hybrid-vdW interaction can be formed, playing a key role in forming the HVE. Owing to this unique hybrid-vdW interaction, the deposit can effectively wet the substrate without a lattice match requirement [Fig. 1(d)]. Meanwhile, since the vdW gap leaves the high unsaturation of a non-vdW epilayer, the growth tendency in the out-of-plane direction is significantly larger than that of the FV or VE model. As a result, the growth in plane and out of plane occurs simultaneously. The L and h of the epilayer are strongly correlated in the HVE model, different from the existing models [Fig. 1(f)].

First epilayer growth—We select AlN grown on graphene with the (0001) surface as a representative case to

demonstrate the HVE model. For the standard growth process, the steps of adatom adsorption-diffusion, nucleation, and growth have been extensively studied (the details of first epilayer growth can be found in Figs. S1-S13 of Sec. I in the Supplemental Material [31]). Overall, for the first epilayer, the shape of growth island is determined by the symmetry: When the symmetry of the substrate (graphene) and epilayer [AlN(0001) plane] is C_{6v} and C_{3v} , respectively, the shape of the epilayer will satisfy the C_{3v} symmetry [32]. Interestingly, the formation energy of the N-terminated zigzag edge (NZE) (~ 3.71 eV/atom) is significantly larger than that of the Al-terminated zigzag edge (AlZE) (~ 0.62 eV/atom), indicating that, for the first epilayer, the island with AlZE prefers to form during growth (Fig. S7 in the Supplemental Material [31]). As shown in Fig. 2(a), to reveal the growth mechanism of HVE, a triangular island with AlZE is performed to capture the major features.

During the in-plane growth, owing to the chemical inertness of a graphene surface, the chemical bonds between the central area of nitride thinfilm and graphene will spontaneously break, and only the N atoms at the corner of an AlN island can form chemical bonds with the substrate [Fig. 2(a)], no matter what size of the island [Fig. 2(b)]. Except for these corner N atoms, there is a vdW gap with a distance of about 3 Å in the central region between first epilayer and graphene, forming an interesting hybrid-vdW interaction [Fig. 2(b)]. This can effectively lift the requirement of the lattice match between the AlN

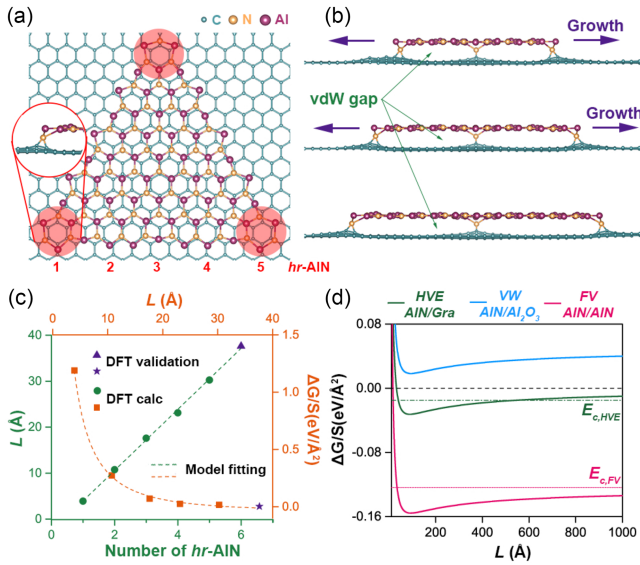


FIG. 2. First epilayer growth. (a) Structure of Al-terminated triangular AlN island on graphene, formed by five AlN hexagonal ring (hr AlN) along the edge (Fig. S10 in the Supplemental Material [31]). Shaded regions indicate the formation of chemical bonds between AlN and graphene around the corner sites. (b) Top to bottom: side views of AlN islands with edge lengths of 4, 5, and 6 hr AlN rings during in-plane growth, respectively. (c) Edge length as a function of hr AlN (green) and formation energy per area as a function of edge length for the first AlN epilayer (orange). Orange squares and green circles are DFT-calculated results, which are used to fit the continuum model (dashed lines). Purple pentagons and purple triangles are calculated by DFT to verify our fitted model. (d) Formation energy per area for the first epilayer as a function of island size for HVE, FV, and VW models, which are simulated by triangular epilayers on graphene, AlN(0001) and Al₂O₃(0001) surfaces, respectively. Formation energy of AlN along the out-of-plane direction in HVE ($E_{c,HVE}$) and FV ($E_{c,FV}$) models is also plotted here for comparison.

epilayer and graphene. The imbalanced stress occurs solely at the corner site and will not increase as the island becomes larger, i.e., this stress can be treated as a constant. Consequently, to reveal the growth mechanism, we can construct a continuum model to calculate the island formation energy ΔG , which can be written as

$$\Delta G = E_{\text{edge-surface}} + E_{\text{elastic}} + E_{\text{binding}}, \quad (1)$$

where $E_{\text{edge-surface}}$ is the energy cost for forming the edge (surface) for the 2D (3D) case. E_{elastic} is the interaction energy induced by elastic forces on the edge or surface, including the interaction between point forces and force monopoles. E_{binding} is the energy for binding the epilayer to the substrate, which plays a critical role to distinguish different growth models.

For HVE growth, the E_{binding} can be written as a constant for approximation [Fig. 1(e)]. Based on the formula

derivation (see details in Method in the Supplemental Material [31]), we can obtain the formation energy of the first epilayer per area for the HVE model as

$$\frac{\Delta G}{S} = \frac{1}{L} \left(C_1 - C_2 \ln \frac{L}{ea_0} + \frac{C_3}{L} \right), \quad (2)$$

where C_1 , C_2 , and C_3 are constants related to Young's modulus, the Poisson ratio, edge energy, and energy cost by stress in the corners. L is the length of the island, and a_0 is the cutoff length below which the continuum theory is no longer suitable [42]. The parameters in Eq. (2) can be fitted by the density functional theory (DFT) calculations (see Table S1 in the Supplemental Material [31]). As shown in Fig. 2(c), L shows a good linearity with the number of AlN hexagonal rings, indicating that the growth island has the same triangular shape with the increase of size. Meanwhile, the additional DFT-calculated values for L and $(\Delta G/S)$ also well verify the model. As shown in Fig. 2(d), when $(\Delta G/S)$ reduces to zero, the L_0 is solved to be 32.37 Å. This means that when $L < L_0$, the process of nucleation costs energy; when $L > L_0$, the island will grow irreversibly. Interestingly, when the length reaches $L_{\text{min}} = 89.57$ Å, the $(\Delta G/S)$ reaches a minimum, which indicates that the island will be energetically most favorable. When L is further increased to about 1 mm (Fig. S11 in the Supplemental Material [31]), $(\Delta G/S)$ is close to zero again, which means that the first epilayer can be grown as large as 1 mm. In practice, the size of islands can be controlled by specific growth conditions (Fig. S12 in the Supplemental Material [31]).

For comparison, we also select the homogeneous AlN epilayer on AlN(0001) and heterogeneous AlN epilayer on Al₂O₃(0001) to simulate the FV and VW models, respectively (Fig. S13 in the Supplemental Material [31]). In these simulations, the major difference of $(\Delta G/S)$ comes from the E_{binding} term in Eq. (1), $E_{\text{binding}} = \alpha L^2$, where α is the binding coefficient. For the FV model, the AlN epilayer is strong bonded with the AlN(0001) substrate, leading to a large negative binding coefficient $\alpha = -0.124$ eV/Å². Therefore, when the size of the epilayer increases, $(\Delta G/S)$ is always negative, preferring an in-plane growth [Fig. 2(d)]. However, for the VW model, there is a large lattice mismatch (about 20%) between AlN epilayer growth and Al₂O₃(0001) substrate, which leads to a positive binding coefficient, $\alpha = 0.023$ eV/Å². As a result, $(\Delta G/S)$ is always positive, which means in-plane growth is energetically unfavorable [Fig. 2(d)]. Consequently, the 3D islands instead of a continuous thinfilm will be formed.

Out-of-plane growth—Since the vdW gap leaves a high unsaturation (free bonds at the center of island) of the non-vdW epilayer, the growth tendency in the out-of-plane direction is significantly larger than that of the FV or VE model. While the free bonds at the center of the island mainly affect the growth of subsequent layers, the excess charge at the corners will influence the island-substrate

interaction. To reveal the process of the growth in the out-of-plane direction, the steps of adatom climbing, diffusion, nucleation, and growth along the out-of-plane direction have also been extensively investigated (the details of out-of-plane growth can be found in Figs. S14-S19 of Sec. II in the Supplemental Material [31]). The calculated out-of-plane formation energy (E_c) for AlN is $-0.013 \text{ eV}/\text{\AA}^2$ and $-0.124 \text{ eV}/\text{\AA}^2$ in HVE and FV growth, respectively. As shown in Fig. 2(d), the values of out-of-plane and in-plane formation energy are very comparable in the HVE model, indicating that growth can be carried out along both directions simultaneously. Meanwhile, the small energy barriers of adatom climbing from underneath the graphene to the first epilayer and diffusion on the epilayer make the out-of-plane growth kinetically favorable (Fig. S14 in the Supplemental Material [31]). On the other hand, for the FV model, because $(\Delta G/S)$ is always much lower than that of out-of-plane $E_{c,\text{FV}}$, the in-plane growth is always more energetically favorable.

While the shape of the first epilayer on the graphene is triangular, interestingly, it converts to hexagonal starting from the second epilayer (Fig. S17 in the Supplemental Material [31]). This is mainly because the N ZEs that are energetically unstable in the first AlN epilayer become stable in the second AlN epilayer. The shape and size of the second epilayer can be determined by Wulff construction [43,44]. The energy cost in the HVE model mainly comes from the stress in the corners, and the out-of-plane growth is largely independent of the interaction of substrate. In particular, the edge length and number of epilayers in the [0001] direction with the optimal state can be solved and written as

$$\frac{3a_s(E_a - 2E_b)V}{-3a_s^2 + L^2} + \frac{3E_bLV}{-3a_s^2 + L^2} - \frac{3\sqrt{3}}{4}a_s^2E_c \left(-1 + \frac{V}{-3a_s^2 + L^2} \right) + \frac{\sqrt{3}}{4}L^2E_c \left(-1 + \frac{V}{-3a_s^2 + L^2} \right) = 0, \quad (4)$$

where a_s indicates the energetically favorable edge length of Al ZE (see Method for details in the Supplemental Material [31]). The model for the growth in the [0001] direction is fitted with our DFT-calculated results well (Fig. S18 in the Supplemental Material [31]). Interestingly, as shown in Figs. 3(a) and 3(b), at different V , the formation energy is strongly dependent on L and R , which means that the in-plane and out-of-plane growth are strongly correlated. For a given V , we can obtain the energetically favorable h_{\min} , L_{\min} , and R_{\min} . Importantly, at different growth stages with different V , Eqs. (3) and (4) will give rise to different h_{\min} , L_{\min} , and R_{\min} . For example, at the initial growth stage with small V [Fig. 3(a)], the $L_{\min} = 22.9 \text{ \AA}$ and $R_{\min} = 1.00$ (i.e., 3/3); however, at a later growth stage with large V [Fig. 3(b)], L_{\min} is greatly enlarged to 875.0 \AA and R_{\min} is reduced to 0.6, indicating a shape change. The change of shape R mainly results from

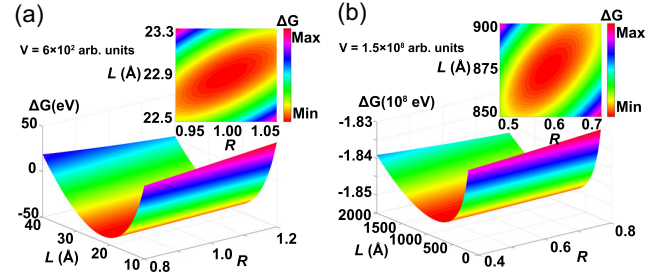


FIG. 3. Out-of-plane growth. Model-calculated formation energy as a function of both R and L at the deposition volumes of (a) $V = 6 \times 10^2$ arb. units and (b) $V = 1.5 \times 10^8$ arb. units for thin and thick AlN epilayers, respectively. Insets show the enlarged area around the minimum of ΔG .

$$\Delta G = (3aE_a + 3bE_b)n_h + (n_h - 1)SE_c, \quad (3)$$

where E_a and E_b are the edge/surface energy of Al ZEs and N ZEs per area and layer, respectively. a and b are the edge lengths of these two kinds of edges, satisfying $a + 2b = L$. The aspect ratio R can be defined as b/a , which is related to the shape of the island. n_h is the number of epilayers in out of plane, which is related to the thickness as $h = n_h \times c$ (c is the distance between epilayers). S and E_c are the area of the hexagonal epilayers and interlayer binding energy per area per layer between the two epilayers, respectively. When the formation energy reaches the minimum, the following equations should be satisfied: $(\partial \Delta G / \partial a) = 0$ and $(\partial \Delta G / \partial h) = 0$. For a given deposition area-volume $V = hS(L, R) = \text{constant}$, a can be solved by the equation

the difference of interlayer binding energy in the out-of-plane direction, which is related to the deposition volume V (Fig. S19 in the Supplemental Material [31]). Again, the unusual growth feature, the strong correlation between L and h , mainly comes from the specific interfacial binding energy. We note that the potential distortions, i.e., structural distortion or defects, in the lower layers of AlN might influence the out-of-plane growth, altering the L and h curves; however, the HVE model developed here could be general and valid.

Experimental verification—To confirm our proposed HVE model, we have performed experimental measurements on the AlN island grown on graphene. First, the single-crystalline graphene was grown by chemical vapor deposition and then transferred to the SiO_2/Si substrates. Second, the graphene/ SiO_2/Si templates were loaded to a MOCVD reactor for the growth of AlN nuclei (more details

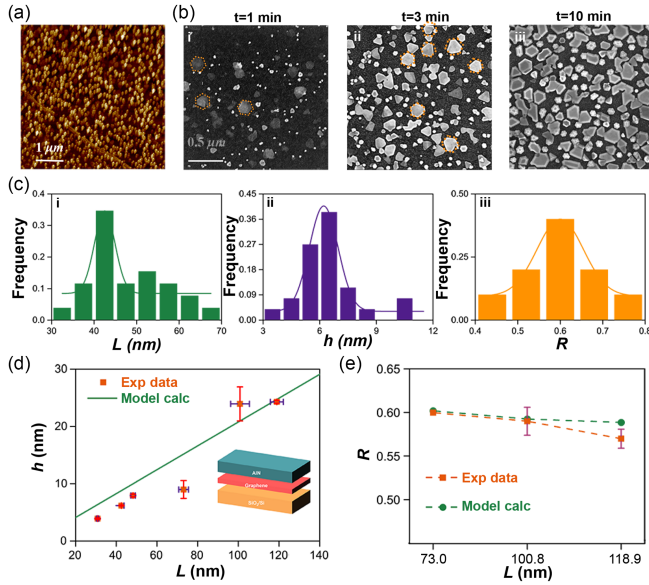


FIG. 4. Experimental verification. (a) AFM image at 4 sec. (b) SEM images of AlN nuclei at 1 min, 3 min, and 10 min (i to iii), respectively. (c) Statistical analysis of L and h at 8 sec as an example, and the R at 1 min as an example (i and ii to iii), respectively. (d) Statistical results of the relationship between L and h in the AlN[0001] direction. Inset: schematic diagram of AlN epilayer grown on the graphene/SiO₂/Si substrate. (e) Statistical distribution of R under different L .

can be found in Method and Sec. III in the Supplemental Material [31]). Both the atomically resolved annular bright-field scanning transmission electron microscopy image and the atomically resolved STEM image of the AlN nuclei indicate that the AlN nuclei show a good single crystalline (Fig. S20 in the Supplemental Material [31]).

For all time points (from 4 s to 10 min), the in-plane edge length and thickness in the [0001] direction are measured by using atomic force microscopy (AFM), as shown in Fig. 4(a). Scanning electron microscopy (SEM) is used to investigate the evolution of the surface morphology and aspect ratios of NZEs and AlZEs under three different growth times (1, 3, and 10 min), as shown in Fig. 4(b) (i to iii), respectively. Furthermore, a statistical analysis of the relationship between h , L , and R for these islands can be obtained, as plotted in Fig. 4(c) (i to iii), (Figs. S21, S22 in the Supplemental Material [31]). Consequently, the relationship between L and h and between L and R can be plotted, as shown in Figs. 4(d) and 4(e), respectively. In general, these data can be well fitted by our model in Eq. (4). For example, for the in-plane L between 20 and 140 nm, the [0001] thickness h almost linearly depends on the L [Fig. 4(d)]. The islands of the highest frequency have an aspect ratio of about 0.6 for almost all time points, which agrees with the value (about 0.61) determined by our theoretical model [Fig. 4(e)]. Again, these available experimental data support the key feature of the HVE model, that is, the in-plane and out-of-plane growth are strongly correlated.

Outlook and summary—We note that whereas the development of the HVE model in the present study is mainly focused on the initial growth of an individual island, another important process is the coalescence of islands forming a continuous sheet. In the latter process, the substrate below graphene may play a key role in forming a continuous single-crystalline film but in a case-by-case way [5–8]. Importantly, our HVE model may still be valid in consideration of the island coalescence (see Figs. S23 and S24 of Sec. VI in the Supplemental Material [31]). In addition, we find that the HVE model can also be applied to describe other similar systems, such as GaN grown on h -BN (see Fig. S25 of Sec. V in the Supplemental Material [31]). Interestingly, since the E_a , E_b , and E_c in the HVE model may be tunable for different non-vdW-vdW systems, our study provides a way to control the L and h and R relationship for diverse device applications.

In summary, we propose that the growth of a nitride epilayer on a vdW substrate belongs to the HVE model. The atomic-scale simulations demonstrate a unique interfacial hybrid-vdW interaction that can be created between AlN and graphene, and, consequently, a first-principles-based continuum growth model reveals that the in-plane and out-of-plane growth is strongly correlated, which is absent in the existing growth models. The concept of HVE is further confirmed by our experimental measurements, opening a new way to control the shape and thickness of nitrides.

Acknowledgments—This work was supported by the National Natural Science Foundation of China (Grants No. 12274024 and No. 12088101), the National Key Research and Development Program of China (Grants No. 2022YFA1405600 and No. 2022YFA1402401), and NSAF (Grant No. U2230402). L. H. is also thankful for the support of the Beijing Institute of Technology Research Fund Program for Young Scholars. We also acknowledge the computing resources of HPC clusters at BIT and the Tianhe-2-JK cluster at CSRC.

B. H. convinced this project. L. H. performed all the computations. D. L., X. Y., and B. S. carried the epitaxial growth and characterization. L. H., X. Y., and B. H. analyzed data. L. H. and B. H. wrote the manuscript with the help of other authors.

- [1] R. Yan, G. Khalsa, S. Vishwanath, Y. Han, J. Wright, S. Rouvimov, D. S. Katzer, N. Nepal, B. P. Downey, D. A. Muller *et al.*, GaN/NbN epitaxial semiconductor/superconductor heterostructures, *Nature (London)* **555**, 183 (2018).
- [2] Y. Kobayashi, K. Kumakura, T. Akasaka, and T. Makimoto, Layered boron nitride as a release layer for mechanical transfer of GaN-based devices, *Nature (London)* **484**, 223 (2012).

- [3] T. A. Chen, C. P. Chuu, C. C. Tseng, C. K. Wen, and L. J. Li, Wafer-scale single-crystal hexagonal boron nitride monolayers on Cu(111), *Nature (London)* **579**, 219 (2020).
- [4] K. Chung, C.-H. Lee, and G.-C. Yi, Transferable GaN layers grown on ZnO-coated graphene layers for optoelectronic devices, *Science* **330**, 655 (2010).
- [5] Y. Kim, S. S. Cruz, K. Lee, B. O. Alawode, C. Choi, Y. Song, J. M. Johnson, C. Heidelberger, W. Kong, S. Choi *et al.*, Remote epitaxy through graphene enables two-dimensional material-based layer transfer, *Nature (London)* **544**, 340 (2017).
- [6] W. Kong, H. Li, K. Qiao, Y. Kim, K. Lee, Y. Nie, D. Lee, T. Osadchy, R. J. Molnar, D. K. Gaskill *et al.*, Polarity governs atomic interaction through two-dimensional materials, *Nat. Mater.* **17**, 999 (2018).
- [7] J. Kim, C. Bayram, H. Park, C.-W. Cheng, C. Dimitrakopoulos, J. A. Ott, K. B. Reuter, S. W. Bedell, and D. K. Sadana, Principle of direct van der Waals epitaxy of single-crystalline films on epitaxial graphene, *Nat. Commun.* **5**, 4836 (2014).
- [8] H. Kim, K. Lu, Y. Liu, H. S. Kum, K. S. Kim, K. Qiao, S.-H. Bae, S. Lee, Y. J. Ji, K. H. Kim *et al.*, Impact of 2D–3D heterointerface on remote epitaxial interaction through graphene, *ACS Nano* **15**, 10587 (2021).
- [9] D. Liu, L. Hu, X. Yang, Z. Zhang, H. Yu, F. Zheng, Y. Feng, J. Wei, Z. Cai, Z. Chen *et al.*, Polarization-driven-orientation selective growth of single-crystalline III-nitride semiconductors on arbitrary substrates, *Adv. Funct. Mater.* **32**, 2113211 (2022).
- [10] Q. Chen, K. Yang, B. Shi, X. Yi, J. Wang, J. Li, and Z. Liu, Principles for 2D-material-assisted nitrides epitaxial growth, *Adv. Mater.* **35**, 2211075 (2023).
- [11] F. Liu, T. Wang, Z. Zhang, T. Shen, X. Rong, B. Sheng, L. Yang, D. Li, J. Wei, S. Sheng *et al.*, Lattice polarity manipulation of quasi-vdW epitaxial GaN films on graphene through interface atomic configuration, *Adv. Mater.* **34**, 2106814 (2022).
- [12] D. Jang, C. Ahn, Y. Lee, S. Lee, H. Lee, D. Kim, Y. Kim, J.-Y. Park, Y.-K. Kwon, J. Choi *et al.*, Thru-hole epitaxy: A highway for controllable and transferable epitaxial growth, *Adv. Mater. Interfaces* **10**, 2201406 (2023).
- [13] F. Ponce and D. Bour, Nitride-based semiconductors for blue and green light-emitting devices, *Nature (London)* **386**, 351 (1997).
- [14] P. Waltereit, O. Brandt, A. Trampert, H. Grahn, J. Menniger, M. Ramsteiner, M. Reiche, and K. Ploog, Nitride semiconductors free of electrostatic fields for efficient white light-emitting diodes, *Nature (London)* **406**, 865 (2000).
- [15] Z. Zheng, L. Zhang, W. Song, S. Feng, H. Xu, J. Sun, S. Yang, T. Chen, J. Wei, and K. J. Chen, Gallium nitride-based complementary logic integrated circuits, *Nat. Electron.* **4**, 595 (2021).
- [16] Y. Sun, K. Zhou, Q. Sun, J. Liu, M. Feng, Z. Li, Y. Zhou, L. Zhang, D. Li, S. Zhang *et al.*, Room-temperature continuous-wave electrically injected InGaN-based laser directly grown on Si, *Nat. Photonics* **10**, 595 (2016).
- [17] M. C. Sequeira, J.-G. Mattei, H. Vazquez, F. Djurabekova, K. Nordlund, I. Monnet, P. Mota-Santiago, P. Kluth, C. Grygiel, S. Zhang *et al.*, Unravelling the secrets of the resistance of GaN to strongly ionising radiation, *Commun. Phys.* **4**, 51 (2021).
- [18] M. C. Sequeira, F. Djurabekova, K. Nordlund, J.-G. Mattei, I. Monnet, C. Grygiel, E. Alves, and K. Lorenz, Examining different regimes of ionization-induced damage in GaN through atomistic simulations, *Small* **18**, 2102235 (2022).
- [19] V. M. Kaganer, B. Jenichen, R. Shayduk, W. Braun, and H. Riechert, Kinetic optimum of Volmer-Weber growth, *Phys. Rev. Lett.* **102**, 016103 (2009).
- [20] A. C. Levi and M. Kotrla, Theory and simulation of crystal growth, *J. Phys. Condens. Matter* **9**, 299 (1997).
- [21] D. Díaz-Fernández, J. Méndez, F. Yubero, G. Domínguez-Cañizares, A. Gutiérrez, and L. Soriano, Study of the early stages of growth of Co oxides on oxide substrates, *Surface Interface Anal.* **46**, 975 (2014).
- [22] K. Murano and K. Ueda, Surfactant effect of hydrogen for nickel growth on Si(111) 7×7 surface, *Surf. Sci.* **357**, 910 (1996).
- [23] Z. Y. Hang and C. V. Thompson, Grain growth and complex stress evolution during Volmer–Weber growth of polycrystalline thin films, *Acta Mater.* **67**, 189 (2014).
- [24] A. Baskaran and P. Smereka, Mechanisms of Stranski-Krastanov growth, *J. Appl. Phys.* **111**, 044321 (2012).
- [25] M. Heiss, Y. Fontana, A. Gustafsson, G. Wüst, C. Magen, D. O’regan, J. Luo, B. Ketterer, S. Conesa-Boj, A. Kuhlmann *et al.*, Self-assembled quantum dots in a nanowire system for quantum photonics, *Nat. Mater.* **12**, 439 (2013).
- [26] T. Walther, A. G. Cullis, D. J. Norris, and M. Hopkinson, Nature of the Stranski-Krastanow transition during epitaxy of InGaAs on GaAs, *Phys. Rev. Lett.* **86**, 2381 (2001).
- [27] A. Koma, K. Sunouchi, and T. Miyajima, Fabrication and characterization of heterostructures with subnanometer thickness, *Microelectron. Eng.* **2**, 129 (1984).
- [28] Y. Shi, W. Zhou, A.-Y. Lu, W. Fang, Y.-H. Lee, A. L. Hsu, S. M. Kim, K. K. Kim, H. Y. Yang, L.-J. Li *et al.*, van der Waals epitaxy of MoS₂ layers using graphene as growth templates, *Nano Lett.* **12**, 2784 (2012).
- [29] F. Ohuchi, B. Parkinson, K. Ueno, and A. Koma, van der Waals epitaxial growth and characterization of MoSe₂ thin films on SnS₂, *J. Appl. Phys.* **68**, 2168 (1990).
- [30] K. Yan, H. Peng, Y. Zhou, H. Li, and Z. Liu, Formation of bilayer bernal graphene: Layer-by-layer epitaxy via chemical vapor deposition, *Nano Lett.* **11**, 1106 (2011).
- [31] See Supplemental Material at <http://link.aps.org/supplemental/10.1103/PhysRevLett.133.046102> for more details about computational methods of DFT, MD, derivation of our developed continuum model of growth and experimental characterization, details of growth process in plane, out-of-plane and statistical results of experimental observation, which includes Refs. [9,12,32–41].
- [32] J. Dong, L. Zhang, X. Dai, and F. Ding, The epitaxy of 2D materials growth, *Nat. Commun.* **11**, 5862 (2020).
- [33] G. Kresse and J. Hafner, *Ab initio* molecular-dynamics simulation of the liquid-metal–amorphous-semiconductor transition in germanium, *Phys. Rev. B* **49**, 14251 (1994).
- [34] J. P. Perdew, K. Burke, and M. Ernzerhof, Generalized gradient approximation made simple, *Phys. Rev. Lett.* **77**, 3865 (1996).

- [35] S. Grimme, Semiempirical GGA-type density functional constructed with a long-range dispersion correction, *J. Comput. Chem.* **27**, 1787 (2006).
- [36] G. Henkelman, B. P. Uberuaga, and H. Jónsson, A climbing image nudged elastic band method for finding saddle points and minimum energy paths, *J. Chem. Phys.* **113**, 9901 (2000).
- [37] Y. Kangawa, T. Ito, A. Taguchi, K. Shiraishi, and T. Ohachi, A new theoretical approach to adsorption-desorption behavior of Ga on GaAs surfaces, *Surf. Sci.* **493**, 178 (2001).
- [38] Y. Feng, X. Yang, Z. Zhang, D. Kang, J. Zhang, K. Liu, X. Li, J. Shen, F. Liu, T. Wang *et al.*, Epitaxy of single-crystalline GaN film on CMOS-compatible Si(100) substrate buffered by graphene, *Adv. Funct. Mater.* **29**, 1905056 (2019).
- [39] Z. Zhang and M. G. Lagally, Atomistic processes in the early stages of thin-film growth, *Science* **276**, 377 (1997).
- [40] V. I. Artyukhov, Y. Liu, and B. I. Yakobson, Equilibrium at the edge and atomistic mechanisms of graphene growth, *Proc. Natl. Acad. Sci. U.S.A.* **109**, 15136 (2012).
- [41] R. F. Sekerka, Equilibrium and growth shapes of crystals: How do they differ and why should we care?, *Cryst. Res. Technol.* **40**, 291 (2005).
- [42] F. Liu, Modeling and simulation of strain-mediated nanostructure of formation on surface, in *Handbook of Theoretical and Computational Nanotechnology*, edited by M. Rieth and W. Schommers (American Scientific Publishers, Valencia, 2006), Vol. 4, pp. 577–625.
- [43] Z. Zhang, A. J. Mannix, X. Liu, Z. Hu, N. P. Guisinger, M. C. Hersam, and B. I. Yakobson, Near-equilibrium growth from borophene edges on silver, *Sci. Adv.* **5**, eaax0246 (2019).
- [44] W.-K. Burton, N. t. Cabrera, and F. Frank, The growth of crystals and the equilibrium structure of their surfaces, *Phil. Trans. R. Soc. A* **243**, 299 (1951).